

Model Slicing for Supporting Complex Analytics with Elastic Inference Cost and Resource Constraints

Shaofeng Cai[†], Gang Chen[§], Beng Chin Ooi[†], Jinyang Gao[‡]

[†]National University of Singapore
{shaofeng, ooi bc}@comp.nus.edu.sg

[§]Zhejiang University
cg@zju.edu.cn

[‡]Alibaba Group
jinyang.gjy@alibaba-inc.com

ABSTRACT

Deep learning models have been used to support analytics beyond simple aggregation, where deeper and wider models have been shown to yield great results. These models consume a huge amount of memory and computational operations. However, most of the large-scale industrial applications are often computational budget constrained. Current solutions are mainly based on model compression – deploying a smaller model to save the computational resources. Meanwhile, the peak workload of inference service could be 10x higher than the average cases, with even unpredictable extreme cases. Lots of computational resources could be wasted during off-peak hours. On the other hand, the system may crash when the workload exceeds system design. Supporting such deep learning service with dynamic workload cost-efficiently remains to be a challenging problem. In this paper, we address this conflict with a general and novel training scheme called *model slicing*, which enables deep learning models to provide predictions within prescribed computational resource budget dynamically. *Model slicing* could be viewed as an elastic computation solution without requiring more computation resources, but by slightly sacrificing prediction accuracy. In a nutshell, partially ordered relation is introduced to the basic components of each layer in the model, namely neurons in dense layers and channels in convolutional layers. Specifically, if one component participates in the forward pass, then all of its preceding components are also activated. Dynamically trained under such structural constraint, we can slice a narrower sub-model during inference whose run-time memory and computational operation consumption is roughly quadratic to the width controlled by a single parameter *slice rate*. Extensive experiments on NNLM and CNNs show that models trained with *model slicing* can support on demand workload with elastic inference cost effectively with minimum performance loss.

1. INTRODUCTION

Database management systems (DBMS) have been widely used and optimized to support OLAP-style analytics. In order to better understand the data and decipher the information that truly counts in the era of Big Data for its ever-increasing data size and complexity, many advanced large-scale machine learning models have been devised, from million-dimension linear models (e.g. Logistic Regression [40], feature selection [54]) to complex models like Deep Neural Networks [30]. To meet the demand for more complex analytic queries, most OLAP database vendors are integrating Machine Learning (ML) libraries into their systems (e.g. SQL

Server pymssql¹, DB2 python.ibm.db² and etc). Such integrated ML analytics are generally much more effective since the ML task is treated as one part of the query plan rather than an individual black-box system. Based on the higher-level abstraction, lots of optimization can be adopted. For example, query planning [42, 31], lazy evaluation [56], materialization [54] and operator optimization [1] could be considered in a fine-grained manner.

Cost and accuracy are always the two most crucial criteria considered for analytic tasks. Lots of research on approximate query processing have been conducted [33, 4] to provide faster yet approximate analytical query results in modern large-scale analytical database systems, yet such trade-off is not equally well researched for modern ML analytic tasks, particularly deep neural network models. There are two characteristics of the inference cost of analytic tasks for deep neural network models. Firstly, with the development of high-end hardware and large-scale datasets, recent deep models are growing deeper [30, 15] and wider [52, 51]. State-of-the-art models have been designed with up to hundreds of layers and tens of millions of parameters, which leads to a dramatic increase of the inference cost. For instance, a 152-layer ResNet [15] with over 60 million parameters requires up to 20 Giga FLOPs for the inference of one single 224×224 image. The surging computational cost severely affects the viability of many deep models in industry-scale applications. Secondly, for most of the analytic tasks, the workload is usually not constant, e.g. the number of images per query for person re-id [57] service in peak hours could be five times more than the workload in the off-peak hours. Therefore, such trade-off should be naturally supported in the inference phase rather than the training phase: using one single deep model with fixed inference cost to support the peak workload could lead to huge amounts of resources wasting in off-peak hours, and may not be able to handle the unexpected extreme workload. How to trade off the accuracy and cost during deep model inference remains a challenging problem of great importance.

Current model architecture re-design [25, 19] or model compression [13, 14, 36] are not able to handle elastic inference satisfactorily, and we shall use an application example to highlight the challenges. Singles' Day shopping festival³ around 11 November was introduced by Taobao.com and is now becoming one of the biggest online shopping festivals

¹<https://docs.microsoft.com/en-us/sql/connect/python/pymssql/python-sql-driver-pymssql>

²<https://github.com/ibmdb/python-ibmdb>

³https://en.wikipedia.org/wiki/Singles%27_Day

around the world. In 2018, the Singles’ Day festival generated close to 30 billion dollars of sales in one single day and had attracted hundreds of millions of users from more than 200 different countries. The peak level of trade rate reached 0.256 million per second, and 42 million processing in the database in the first half hour. In Singles’ Day, the search traffic of the e-commerce search engine increases about three times than in a common day, and could be 10x in its first hour. Meanwhile, the workload of most other services in Alibaba such as OLTP transaction may also hit the peak at the same time [2], and consequently, it is not possible to scale up the service by acquiring more hardware resources from Alibaba Cloud. The system degradation is often executed in two simple and naive approaches: First, some costly deep learning models are replaced by simple GBDT [6, 28] models; Second, the size of the candidate items for ranking is decreased. As a result, the search accuracy suffers dramatically due to the system degradation in such a coarse-grained manner. With a deep learning model supporting elastic inference cost, the system degradation can become much more fine-grained where the inference cost and accuracy trade-off of deep learning model per query sample can be dynamically determined based on the current system workload.

In this paper, instead of constructing small models based on each individual workload requirement, we propose and address a related but slightly different and yet fundamentally important research problem: developing a general framework to support deep learning models with elastic inference cost. We base the framework on a pay-as-you-go model to support dynamic trade-off between computation cost and accuracy during inference time. That is, dynamic optimization is supported based on system workload, availability of resources and user requirements.

We shall examine the aforementioned problem from a fresh system perspective and propose our solution – *model slicing*, a general and novel network training mechanism supporting model inference with elastics cost, to satisfy the runtime memory and computation budget dynamically during the inference phase. The crux of our approach is to impose implicit partially ordered relation on the basic components, namely neurons for the dense layers and channels for the convolutional layers, of each layer in the deep learning model. More specifically, if one component participates in the forward pass of model computation, then all of its preceding components in this layer are also activated under such network topology. Consequently, we can use a single parameter *slice rate* r to control the proportion of components involved in the forward pass of model computation. We empirically share the slice rate among all the layers in the network, thus the computational resources required can be regulated precisely by r . The *slice rate* here is structurally the same concept as width multiplier in [19] which controls the width of the network. However, instead of training only one fixed narrower model as in [19], we train the network in a dynamic manner to preserve the representation ability in all the subnets it contains. For each forward pass during training, as illustrated in Figure 1, we sample the *slice rate* from a predetermined distribution F , and train the corresponding sub-layers.

Such training scheme can be scrutinized under the perspective of residual learning [15, 16] and knowledge distillation [17]. Under such random training process, output components need to build up the representation increasingly,

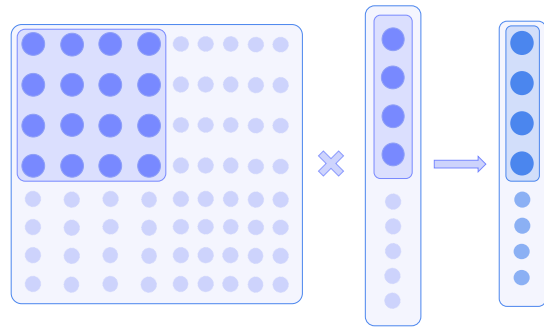


Figure 1: *Model slicing*: slice a sub-layer that is composed of preceding components of the full layer controlled by the *slice rate* r during each forward pass. Only the activated parameters and components of the current layer are required in memory and participate in computation. We illustrate with *slice rate* $r = 0.45$ in a dense layer.

where the preceding components carry the most fundamental information and the trailing components the residual representation relatively. Structurally, the final learned network is an ensemble of R subnets, with R being the number of all valid slice rates. The parameters of these subnets are tied together and during each forward training pass, one subnet uniquely indexed by the slice rate is selected and trained. We conjecture that the accuracy of the resulting full trained network can slightly surpass or at least be comparable to the network trained conventionally. Meanwhile, smaller subnets gradually distill knowledge from larger subnets as the training progresses. Therefore, we can readily slice a subnet out of the full network with minimum accuracy degradation.

Our proposed training scheme is novel and has many advantages over existing methods in various scenarios, in particular model compression, model cascade and anytime prediction. First, *model slicing* is readily applicable to existing neural networks, requiring no iterative retraining and dedicated library/hardware support like most compression methods [14, 36]. Second, instead of training a set of models and optimize the scheduling of these models with different accuracy-cost trade-off as is in conventional model cascade [27, 47], *model slicing* provides the same functionality of producing an approximate low-cost prediction with only one model, meanwhile reuse the computation to the largest extent. Third, the structure of the model trained with *model slicing* naturally supports applications where the model is required to give prediction within given computational budget dynamically, i.e. anytime prediction [21, 20].

Our main technical contributions are:

- We develop a general training and inference framework *model slicing* that enables deep neural network models to support complex analytics with the elastic trade-off between accuracy and inference cost/resource constraints on a per-input basis.
- We formally introduce *model slicing* to general neural network models and further convolutional and recurrent neural networks. We also study the training details of *model slicing* and their impact in depth.
- We empirically validate through extensive experiments that trained with *model slicing*, neural networks can

approach the performance of an ensemble of networks with one single model and support fluctuating workload with up to 16x volatility; Two exemplary applications are also introduced to illustrate the usefulness of *model slicing*.

The rest of the paper is organized as follows. Section 2 provides a literature survey of related works. In Section 3, we introduce the *model slicing* approach and how it can be applied to various deep learning models such as Convolutional Neural Networks (CNNs), Recurrent Neural Networks (RNNs) and etc. We then show how *model slicing* can benefit present industrial deep learning service in Section 4 with illustrating applications of system degradation and cascade ranking. Experimental evaluation of *model slicing* are given in Section 5, under prevailing natural language processing and computer vision problem on standard public benchmark datasets. Visualizations and detailed discussions of the results are also provided. Section 6 concludes the paper and points out some further research directions.

2. RELATED WORK

2.1 Resource-aware Model Optimization

Many recent works directly devise networks which are more economical in producing predictions. SkipNet [48] incorporates reinforcement learning into the network design, which guides the gating module for each residual block whether to bypass the corresponding layer. SkipNet can provide predictions more efficiently yet in a less controlled manner inherently. In MoE [41], a gating network is introduced to select a smaller number of networks out a mixture-of-experts which consists of up to thousands of networks during inference for each sample. This kind of model ensemble approach aims to scale up the model capacity without introducing much overhead, while our approach enables each single trained model to scale down, supporting elastic inference cost.

MSDNet [21] supports classification with computational resource limits at test time by inserting multiple classifiers into a 2D multi-scale version of DenseNet [23]. By early-exit into a classifier, MSDNet can provide predictions within the given computation requirement. ANNs [20] adopts a similar design strategy of introducing auxiliary classifiers with Adaptive Loss Balancing, which supports the trade-off between accuracy and computational cost by using the intermediate features. [37] also develop a model that can successively improve prediction quality with each iteration but this approach is uniquely suited for segmenting videos with RNN models. These methods can largely alleviate the computational efficiency problem. However, they are highly specialized networks, which restrict their applicability. Functionally, models trained with *model slicing* also reuse intermediate features and support progressive prediction but with width slicing. *Model slicing* works similarly to these networks yet is more efficient, flexible and general.

2.2 Model Compression

Reducing the model size and computational cost has become a central problem in the deployment of deep learning solutions in real-world applications. Many works have been proposed to resolve the challenges of growing network size and surging resource expenditure incurred, mainly memory

and computation. The mainstream solutions are to compress networks into smaller ones, including low-rank approximation [12], network quantization [10, 13, 14], weight pruning [14, 13], network sparsification on different level of structure [3, 49, 36] etc.

To this end, many model compression approaches attempt to reduce the model size on the trained networks. [12] exploits model redundancy with tensor decomposition on the weight matrix. [10] and [14] instead propose to quantize the network weights to save storage space. HashNet [7] also proposes to hash network weights into different groups and sharing weight values within each group. These techniques are effective in reducing model size. For instance, [14] achieves up to 35x to 49x compression rates on AlexNet [30]. Although a huge amount of storage can be saved, these techniques can hardly reduce run-time memory or inference time, and they typically need a dedicated library and/or hardware support.

Many studies propose to prune weights, filters or channels in the networks. These approaches are generally effective because deep models typically contain a huge amount of redundancy. [13, 14] iteratively prune unimportant connections with small weight values in trained neural networks. [44] further guides the sparsification of neural networks during training by explicitly imposing sparse constraints over each weight with a gate variable. The resulting networks are highly sparse which can be stored compactly in a sparse format. However, the speedup of inference time of these methods depend heavily on dedicated sparse matrix operation libraries or hardware and the runtime memory saving is again very limited since most of the memory consumption comes from the activation maps instead of these weights. [49, 36, 34] reduce the model size more radically by imposing regularization on the channel or filter and prune those components of little contribution. Like *model slicing*, channel and filter level sparsity can reduce the model size, runtime memory footprint and also lower the number of computational operations. Yet these methods require iterative fine-tuning to regain performance and support no inference time control.

2.3 Efficient Model Design

Instead of compressing existing large neural networks during or after training, recent works have also been exploring more efficient network design. ResNet [15, 16] proposes residual learning via the shortcut of identity mapping and efficient bottleneck structure, which enables the training of very deep networks without introducing parameters. [45] shows that ResNet behaves like an ensemble of shallow networks and it can still function normally with a certain fraction of layers being removed. FractalNet [32] contains a repeated application of the fractal architecture with interacting subpaths. FractalNet adopts drop-path training which randomly selects certain paths during training, allowing for the extraction of fixed-depth subnetworks after training without significant performance loss. These network architectures, to some extent, can support on demand workload by slicing subnetworks layer-wise or path-wise. However, they are less generally applicable and the accuracy deteriorates significantly when the network shrinks shorter or narrower.

Many recent works focus on designing lightweight networks. SqueezeNet [25] reduces parameters and computa-

tion with the fire module. MobileNet [19] and Xception [9] utilize depth-wise and point-wise convolution for more parameter efficient convolutional neural networks. ShuffleNet [55] proposes point-wise group convolution with channel shuffle to help the information flowing across the channels. These architectures scrutinize the bottleneck in conventional convolutional neural networks and search for more efficient transformation, reducing the model size and computation greatly.

3. MODEL SLICING

We aim to provide a general training scheme for neural networks to support on demand workload with elastic inference cost. More specifically, the target is to enable the neural network to produce prediction within prescribed computational resources limit dynamically, mainly computational operation C meanwhile preserving the accuracy to the largest extent.

Existing methods of model compression, model ensemble and anytime prediction models can partially address this problem, but each has its limitations. Model compression methods such as *network slimming* [36] which compresses channel width each layer, can produce efficient models while they typically take longer training time for iterative pruning and retraining, and more importantly, have no control over resources required during inference time. Model ensemble methods, e.g. the ensemble of varying depth/networks, can largely support inference time resources control by scheduling the model chosen for the immediate prediction task. However, deploying an ensemble of the models takes several times the amount of disk/memory storage; further, scheduling of these models is a non-trivial task to the system in deployment. Many works [21, 20, 37] instead exploiting intermediate features of the model for faster approximate prediction. For instance, Multi-Scale DenseNet [21] (MSD-Net) inserts multiple classifiers in a multi-scale version of DenseNet [23] and supports anytime prediction with early-exit on the proper classifier when the time budget exhausts.

Our *model slicing* also exploits and reuses intermediate features produced by the model while sidesteps all the aforementioned problems. The key idea is to propose a general training and inference mechanism called *model slicing* which slices a narrower subnet for faster computation. With *model slicing*, neural networks are able to dynamically control the width of the subnet and regulate the computational resource consumption with one single parameter *slice rate*. We compare the performance of ResNet trained with *model slicing* with state-of-the-art models in the setting of anytime prediction in Figure 2. We can observe that model ensemble methods are strong baselines which trade off accuracy for lower inference cost and that the varying width ensemble of ResNet-164 performs better than varying depth, especially in lower budget prediction. The finding demonstrates the superiority of width slicing over depth slicing by inserting multiple classifiers into the network [20, 21]. This is also corroborated by the rapid loss in accuracy of ResNet with Multi-Classifiers (single model) in Figure 2. We will show that trained with model slicing, we are able to approach the performance of the ensemble of varying width networks with one single model.

3.1 Model Slicing for Neural Networks

We shall start by introducing *model slicing* to neural networks of the stacked fully connected layer. Each dense

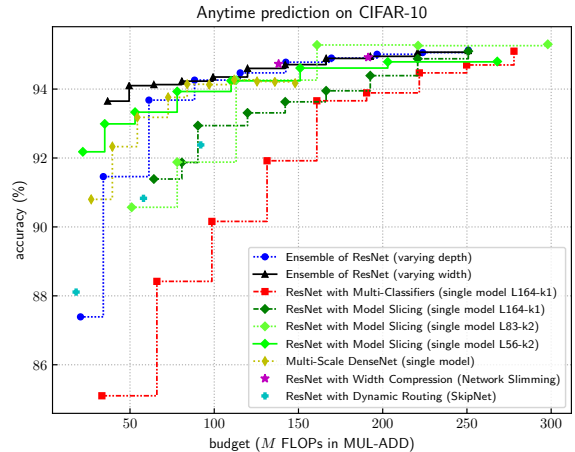


Figure 2: Classification accuracy w.r.t inference FLOPs of ResNet trained with *model slicing* against ensemble, compression and other baselines on the CIFAR-10 dataset in the anytime prediction setting.

layer in the neural network transforms via a weight matrix $\mathbf{W} \in \mathbb{R}^{N \times M}$: $\mathbf{y} = \mathbf{W}\mathbf{x}$, where $\mathbf{x} = [x_1, x_2, \dots, x_M]$, a M -dimension input vector, corresponds to M input neurons and $\mathbf{y} = [y_1, y_2, \dots, y_N]$, N output neurons correspondingly. Details such as the bias and non-linearity are omitted here for brevity. As illustrated in Figure 1, a gating variable is *implicitly* introduced to impose the structural constraint on each input neuron x_j :

$$y_i = \sum_{j=1}^M w_{ij}(\alpha_j \cdot x_j) \quad (1)$$

Each gating variable α_j thus controls the participation of the corresponding neuron x_j in each forward pass during and after training. Formally, the structural constraint is achieved by enforcing partial ordered relation among these gating variables:

$$\forall i \forall j (i, j \in \{1, 2, \dots, M\} \wedge i < j \wedge \alpha_j = 1 \rightarrow \alpha_i = 1) \quad (2)$$

which means the set of all activated neurons during each forward pass in this layer forms a continuous chunk starting from the first neuron. Then the value of all gating variable $\alpha = [\alpha_1, \alpha_2, \dots, \alpha_M]$ can be jointly determined by indexing the rightmost neuron activated with one single parameter *slice rate* $r \in (0, 1]$:

$$\alpha_j = \mathbb{1}(j \leq \text{round}(r \times M)) \quad (3)$$

Empirically, the *slice rate* is shared among all the layers in the network. Thus the width of the whole network can be regulated by this single parameter r . As illustrated in Figure 1, only the sliced part of the weight matrix and components are activated and required to be loaded to memory for inference in the current forward pass. We denote the computational operation required by the full network as C_0 , then the computational operation required by the subnet of

slice rate r , or r -net, is roughly $r^2 \times C_0$. Therefore, the runtime computational resources limit C_t can be dynamically satisfied by restricting slice rate r as Equation 4:

$$r \leq \min(\sqrt{\frac{C_t}{C_0}}, 1) \quad (4)$$

It is worth noting that a subnet can be readily sliced and deployed out of the network trained with *model slicing* whose disk storage and runtime memory consumption are also roughly quadratic to the slice rate r . Besides the constraint of run-time computational resources, another crucial issue is to preserve the accuracy in these subnets to the largest extent. To this end, we propose the *model slicing* training scheme where the slice rate r is sampled from a predetermined scheduling scheme F , and the corresponding r -net is optimized under current mini-batch of training samples. The slice rate r is further restricted between 1.0 and a fixed lower bound lb , whose value satisfies Equation 4 under the most rigorous computational resources limit. We shall examine the impact of the scheduling scheme F and lower bound lb in detail in Section 3.5.

Notice that the parameters of all subnets are tied together and any subnet indexed by a slice rate r subsumes all subnets of smaller slice rates. This training scheme structurally works in a way similar to residual learning [15, 16], where the lb -net forms the base network and provides the most fundamental representation. As r grows, the newly-introduced components in the r -net learn the residual presentation. In the viewpoint of knowledge distillation [17], the r -1 network preserve the capacity of the original model and as the training progresses, each r -net gradually learns the representation from larger subnets and transfers the knowledge to smaller ones. Under such training scheme, we conjecture that the full network can preserve the accuracy, or possibly improve due to the regularization and ensemble effect introduced, and in the meantime, the subnets can gradually pick up the performance by distilling knowledge from larger subnets.

3.2 Convolutional Neural Networks

Model slicing is readily applicable to convolutional neural networks with minor adaptation. The most fundamental operation in CNNs comes from the convolutional layer which can be constructed to represent any given transformation $\mathcal{F}_{conv} : \mathbf{X} \rightarrow \mathbf{Y}$, where $\mathbf{X} \in \mathbb{R}^{M \times W_{in} \times H_{in}}$ is the input with M channels of size $W_{in} \times H_{in}$, $\mathbf{Y} \in \mathbb{R}^{N \times W_{out} \times H_{out}}$ the output likewise. Denoting $\mathbf{X} = [\mathbf{x}_1, \mathbf{x}_2, \dots, \mathbf{x}_M]$ and $\mathbf{Y} = [\mathbf{y}_1, \mathbf{y}_2, \dots, \mathbf{y}_N]$ in vector of channels representation, the parameter set associated with each convolutional layer is a set of filter kernels $\mathbf{K} = [\mathbf{k}_1, \mathbf{k}_2, \dots, \mathbf{k}_N]$. In a way similar to the dense layer, *model slicing* on the convolutional layer can be represented as:

$$\mathbf{y}_i = \mathbf{k}_i * \mathbf{X} = \sum_{j=1}^M \mathbf{k}_i^j * (\alpha_j \cdot \mathbf{x}_j) \quad (5)$$

where $*$ denotes convolution operation, \mathbf{k}_i^j is a 2D spatial kernel associated with i_{th} output channel \mathbf{y}_i and convolves on j_{th} input channel \mathbf{x}_j . Consequently, treating channels in convolutional layers analogously to neurons in dense layers, *model slicing* can be directly applied to CNNs with the same training scheme.

One issue arises when applying *model slicing* to CNNs. Specifically, each convolutional layer is typically coupled with a batch normalization layer [26] to normalize inputs in the batch dimension, which stabilizes mean and variance of the input channels received by each output channel. In the implementation of Equation 6, each batch-norm layer normalizes inputs with the batch mean μ and variance σ and keeps records of running estimates of them which will be directly used after training. Here, γ and β are learnable affine transformation parameters of this batch-norm layer associated with each channel. However, with model slicing, the number of inputs received by a given output channel is no longer fixed, which is instead determined by the slice rate r during each forward pass. Consequently, the mean and variance of the batch-norm layer on the output fluctuate drastically thus one single set of the running estimates is unable to stabilize the distribution of the output channel.

$$\hat{\mathbf{x}} = \frac{\mathbf{x}_{in} - \mu}{\sqrt{\sigma^2 + \epsilon}}; \mathbf{x}_{out} = \gamma \hat{\mathbf{x}} + \beta \quad (6)$$

We propose to address this problem with Group Normalization [50], an adaptation to Batch-norm. Group-norm divides channels into groups and normalizes channels the same way as is in Equation 6 with the only modification that the mean and variance are calculated within each group. Formally, given total number of groups G , the mean μ_g and variance σ_g of g th group are estimated within the set of channels in Equation 7 and shared among all the channels in current group for normalization.

$$\mathcal{S}_g = \{\mathbf{x}_j | \text{floor}(\frac{j-1}{G}) = g\} \quad (7)$$

Group-norm normalizes channels group-wisely instead of batch-wisely, avoiding running estimates of the batch mean and variance in batch-norm, whose error increases rapidly as the batch size decreases. Experiments in [50], which is also validated by our experiments on various network architectures, show that the accuracy of group-norm is fairly stable with respect to the batch size and group number. Besides the stability, another benefit of group-norm is its encouragement for group-wise representation, which is in line with the residual learning effect from model slicing training. To introduce model slicing to CNNs, we only need to replace batch-norm to group-norm following each convolutional layer and slice these two layers together in group granularity.

3.3 Recurrent Neural Networks

Model slicing can also be applied to recurrent layers in a similar manner as is in fully connected layers. Take the vanilla recurrent layer expressed in Equation 8 for demonstration, the difference is that the output \mathbf{h}_t is computed from two sets of inputs, namely \mathbf{x}_t and \mathbf{h}_{t-1} . Consequently, we can slice each input on the recurrent layer separately and follow the same training scheme as fully connected layers.

$$\mathbf{h}_t = \sigma(\mathbf{W}_{hx} \mathbf{x}_t + \mathbf{W}_{hh} \mathbf{h}_{t-1} + \mathbf{b}_h) \quad (8)$$

Model slicing for recurrent layers of RNN variants such as GRU [8] and LSTM[18] works similarly. Dynamic slicing is applied to all inputs and outputs, including hidden/memory states and various gates, regulated by a single parameter slice rate r each layer.

3.4 Residual Learning in Model Slicing

Our *model slicing* training scheme structurally is reminiscent of residual learning proposed in ResNet [15, 16]. In ResNet, a shortcut connection of identity mapping is proposed to forward input to output directly: $\mathbf{Y} = \mathcal{F}_{conv}(\mathbf{X}) + \mathbf{X}$, where during optimization, the convolutional transformation only needs to learn the residual representation on top of input information \mathbf{X} , namely $\mathbf{Y} - \mathbf{X}$. Analogously, networks trained with model slicing learn to accumulate the representation with additional basic components introduced, specifically, neurons in dense layers and channels in convolutional layers.

To demonstrate the residual learning effect in *model slicing*, we take the transformation in a fully connected layer for example, and analyze the relationship between any two sub-layers of *slice rate* r_1 and r_2 with $r_1 < r_2$. We have the transformation of the r_1 -layer as $\mathbf{Y}_1 = \mathbf{W}_1\mathbf{X}_1$ and the transformation of the r_2 -layer $[\tilde{\mathbf{Y}}_1; \mathbf{Y}_2] = \mathbf{W}_2[\mathbf{X}_1; \mathbf{X}_2]$ in block matrix multiplication as:

$$\begin{bmatrix} \tilde{\mathbf{Y}}_1 \\ \mathbf{Y}_2 \end{bmatrix} = \begin{bmatrix} \mathbf{W}_1 & \mathbf{B} \\ \mathbf{C} & \mathbf{D} \end{bmatrix} \cdot \begin{bmatrix} \mathbf{X}_1 \\ \mathbf{X}_2 \end{bmatrix} = \begin{bmatrix} \mathbf{W}_1\mathbf{X}_1 + \mathbf{B}\mathbf{X}_2 \\ \mathbf{C}\mathbf{X}_1 + \mathbf{D}\mathbf{X}_2 \end{bmatrix} \quad (9)$$

Here, \mathbf{X}_2 is the additional input introduced for r_2 -layer and \mathbf{Y}_2 the corresponding supplementary output produced. Suppose $r_2 - r_1 \ll r_1$, which holds true generally, then the residual learning representation can be clarified in two angles. Firstly, the base representation of r_2 -layer $\tilde{\mathbf{Y}}_1 = \mathbf{W}_1\mathbf{X}_1 + \mathbf{B}\mathbf{X}_2 = \mathbf{Y}_1 + \mathbf{B}\mathbf{X}_2$, which is composed of the base representation \mathbf{Y}_1 and the residual representation $\mathbf{B}\mathbf{X}_2$. Secondly, the output \mathbf{Y}_2 also forms the residual representation in another dimension that is supplementary to the base representation $\tilde{\mathbf{Y}}_1$ in the r_2 layer.

The justification for the residual learning effect in *model slicing* is that the base representation of \mathbf{Y}_1 in r_1 -layer is already optimized for the learning task as the training progresses. Therefore, the additional representation introduced to r_2 -layer evolves to form the residual representation, as is corroborated in the visualization in Section 5.4. Furthermore, this residual learning characteristic provides an efficient way to harness the richer representation of r_2 -net based on r_1 -net by the simple approximation of $\tilde{\mathbf{Y}}_1 \approx \mathbf{Y}_1$. With this approximation in every layer of the network, the most computationally heavy features of $\mathbf{W}_1\mathbf{X}_1$ can be reused without re-evaluating, thus the representation of r_2 -layer can be updated by only calculating $\mathbf{C}\mathbf{X}_1 + \mathbf{D}\mathbf{X}_2$ with orders of magnitude lower computational cost.

3.5 Model Slicing Training Details

3.5.1 Output Re-scaling for Model Slicing

One critical training detail is whether to scale inputs by $\frac{M}{\text{round}(r \times M)}$ in each layer to stabilize the mean aggregated information received for each output component. Theoretically and as is also corroborated in experiments, for fully connected layers and recurrent layers, rescaling is essential because each input contributes equally in the final activation and the rescaling compensates for the scale loss from *model slicing*. On the contrary, rescaling actually deteriorates the performance of the convolutional layer because it destabilizes the learning of scaling factors in the coupling normalization layer.

3.5.2 Slice Rate Scheduling Scheme

For each forward pass of model slicing training, the *slice rate* r is sampled from a predetermined scheduling scheme F , bounded within the interval $[lb, 1]$, then rounds to the *nearest valid slice rate*, each of which corresponds to one particular subnet. Formally, *any* scheduling scheme can be described as sampling the *slice rate* r from a Distribution F , which may change as the training progresses depending on the specific scheme adopted. Denoting all valid *slice rate* r as $r_1 = lb, r_2, \dots, r_N = 1$, we have:

$$\begin{cases} p(r_1) = F(\frac{r_1+r_2}{2}) = \int_{-\infty}^{\frac{r_1+r_2}{2}} f(r)dr, & i = 1 \\ p(r_i) = F(\frac{r_i+r_{i+1}}{2}) - F(\frac{r_{i-1}+r_i}{2}) = \int_{\frac{r_{i-1}+r_i}{2}}^{\frac{r_i+r_{i+1}}{2}} f(r)dr, & 1 < i < N \\ p(r_N) = 1 - F(\frac{r_{N-1}+r_N}{2}) = \int_{\frac{r_{N-1}+r_N}{2}}^{+\infty} f(r)dr, & i = N \end{cases} \quad (10)$$

where $f(r)$ is the probability density function, $F(r)$ the cumulative distribution function of F , $p(r_i)$ the probability of i_{th} *slice rate* r being chosen. Therefore, the scheduling scheme F formally can be parameterized with a Categorical Distribution $Cat[p(r_1), p(r_2), \dots, p(r_N)]$. Based on this formulation, we propose three types of scheduling schemes and evaluate them in Section 5.1.2:

- *Dynamic Scheduling*, where r is sampled from a given distribution throughout. We evaluate Uniform Distribution $\mathcal{U}(lb - span, 1 + span)$ and Normal Distribution $\mathcal{N}(mean, var)$ as two representative distributions, with *span, mean, var* being the hyper-parameters.
- *Progressive Dynamic Scheduling*, where r is first fixed to 1 ($p(r_N) = 1$) until p percentage of the total number of training epochs finish, and then dynamically sampled from a distribution F as *Dynamic Scheduling*.
- *Progressive Static Scheduling*, where r monotonically increases from lb to 1 as the training progresses ($p(r_i) = 1$), with the constraint that r increases after the training of corresponding r -net converges whose parameters are then fixed afterward.

4. EXEMPLAR APPLICATIONS

In this section, we demonstrate how the aforementioned *model slicing* can benefit the deployment of deep learning based services. We use *model slicing* as the basic supporting framework to provide the following two fundamental large scale machine learning services for an industrial recommendation system in practical usage.

4.1 Implementing System Degradation

For a service with a dynamic workload, fine-grained system degradation can be implemented straight-forwardly based on *model slicing*. Query samples come as a stream, and there is a general latency requirement. Similar to MSDNet [21], such queries are usually batch processed due to the benefit of vectorized computation. We design and implement an exemplary solution to guarantee the latency and throughput requirement via *model slicing*. Given processing time per sample for the full model t , to satisfy the dynamic latency requirement T and unknown query workload, we can build a mini-batch every $T/2$ time, and utilize the rest $T/2$ time budget for processing: first examine the number of samples n in this batch, and choose the slice rate r satisfying

$nr^2t \leq T/2$ so that the computation time for this batch is within the budget $T/2$. Under such a system design, no computation resource is wasted as the total processing time per mini-batch can be exactly the time interval of the batch input. Meanwhile, all the samples can be efficiently processed within the required latency.

4.2 Implementing Cascade Ranking

Many information retrieval and data mining applications such as search and recommendation need to rank a large set of data items with respect to many user requests in an online manner. There are generally two issues in this process: 1). Effectiveness as how accurate the obtained results in the final ranked list are and whether there are a sufficient number of good results; and 2). Efficiency such as whether the results are obtained in a timely manner from the user perspective and whether the computational costs of ranking is low from the system perspective. For large-scale ranking applications, it is of vital importance to address both issues for providing good user experience and achieving a cost-saving solution.

Cascade ranking [46, 35] is a strategy designed for such trade-off. It utilizes a sequence of prediction functions in different stages with different cost. It can eliminate irrelevant items (e.g., for a query) in the earlier stages with simple features and models, while better discern more relevant items in later stages with more complicated features and models. In general, functions in early stages require low inference cost while functions in later stages require high accuracy.

One critical feature about cascade ranking is that the optimization target for each function may depend on all other functions in different stages [35]. For instance, given a positive item set $\{1, 2, \dots, 7\}$ and we aim to build a cascade ranking solution with 2 stages, suppose that function in stage 2 mis-drop positive item $\{6, 7\}$, a function in stage 1 mis-drop $\{1, 6, 7\}$ is better than a function mis-drop $\{1, 2\}$ though the former has a higher error rate over the whole dataset (in the first case $\{2, 3, 4, 5\}$ are left while in the second case only $\{3, 4, 5\}$ are left). Lots of analysis are given in [46, 5, 35]. Therefore, we expect the prediction of positive items given by functions in different stages to be consistent so that the accumulated false negatives are minimized. Unfortunately, most of the implementations of the ranking/filtering function at each stage for cascade ranking use different model architectures with different parameters, where the results from different models are unlikely to be consistent.

Model slicing would be an ideal solution for cascade ranking. Firstly, it provides the trade-off of model effectiveness and model efficiency in a single model. The ranking functions at different stages can be obtained by simply configuring the inference cost of the model. Secondly, as is also corroborated in Section 5.4 the prediction results of *model slicing* with different inference cost are inherently correlated, since the larger model is actually using the smaller model as the base of its model representation. Therefore, applying *model slicing* naturally guarantees the consistency among different ranking functions of the subnets, which is the key challenge in cascade ranking problem. We shall illustrate the effectiveness and efficiency of *model slicing* in comparison with the traditional solution of cascade models in a simulation of the cascade ranking scenario in Section 5.4.4.

5. EXPERIMENTS

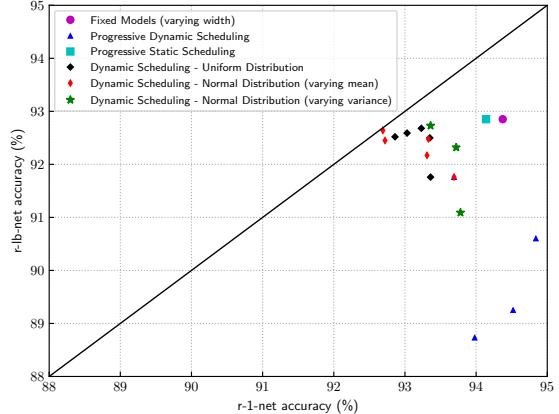


Figure 3: Illustration of the VGG-13 trained with *model slicing* under various training scheduling schemes on CIFAR-10.

We evaluate the performance of *model slicing* on several state-of-the-art neural networks on two categories of public benchmark tasks, specifically NNLM [38, 53, 39] on language modeling and CNNs [43, 15, 52] on image classification. In this section, we first discuss and give details on the experiment setup of *model slicing*. Extensive experiments are then conducted evaluating the performance of *model slicing* in comparison with the baselines. Finally, we examine and visualize the effect of *model slicing* on the network training.

5.1 Model Slicing Setup

5.1.1 Baselines

In the experiments, all the networks trained with *model slicing* are tested with slice rate r from 1 to 0.25 on every $\frac{1}{16}$ and compared primarily with two baselines. The first baseline (*lb 1.0*) is the same network trained without *model slicing*, implemented by fixing *lb* to 1.0 during training. During inference, we slice the first r fraction of each layer in the network for comparison. The second baseline (*fixed models*) is an ensemble of networks of varying width, which generally represents the accuracy upper-bound. In addition to the above two baselines, we also compare model slicing with model compression (Network Slimming [36]), anytime prediction (multi-classifiers methods like MSDNet [21]) and efficient prediction (SkipNet [48]) methods.

5.1.2 Slice Rate Scheduling Scheme

We evaluate the three *slice rate* scheduling schemes proposed in Section 3.5.2 with varying hyper-parameters on VGG-13 and plot the accuracy of the network trained with *model slicing* in the format of (r -1-net accuracy, r -lb-net accuracy) on Figure 3. Among these schemes, Progressive Static Scheduling achieves the best performance whose accuracy is close to the fixed models of varying width, with only minor accuracy loss for the r -1-net; Progressive Dynamic Scheduling generally obtains higher r -1-net accuracy yet with the accuracy decrease in r -lb-net; Dynamic Scheduling, straightforward as it is, strikes a delicate balance between the full network and the smallest subnet. Although Progressive Static Scheduling can achieve higher accuracy that

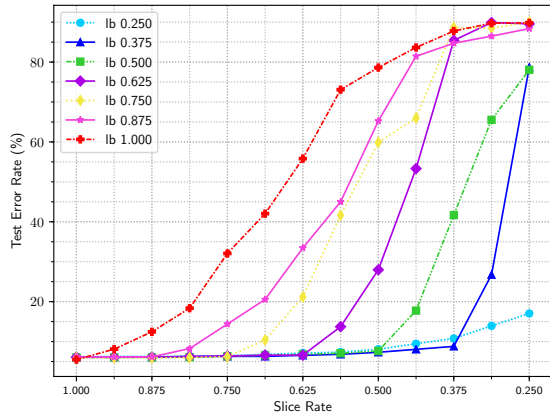


Figure 4: Illustration of the impact of the lower bound lb on the training of VGG-13 with *model slicing* on CIFAR-10.

is comparable to the ensemble of models of varying width with only one model, the training of this scheduling scheme is not efficiently supported by current DL platforms and furthermore, it takes significantly longer training time, which can be up to R times the time of a given model, with R being the number of valid *slice rate*. Therefore, we favor Dynamic Scheduling and empirically, we find out that the normal distribution $\mathcal{N}(1, \frac{1}{3})$ works consistently well, which is thus widely adopted in the experiments with *model slicing* training.

5.1.3 The Lower Bound of Slice Rate

The lower bound lb controls the width of the base network and should at least be set to Equation 4 under the most rigorous limit of computational resources. Figure 4 shows the performance of VGG-13 trained with different lower bounds. Empirically, we find that the accuracy decreases slowly as r decreases towards lb , and networks trained with different lbs perform rather close to each other before their corresponding lbs . For a given lb , however, the accuracy of this corresponding subnet whose r approaches this lb is generally better than others. This is mainly because these subnets are optimized more frequently here. When the slice rate r surpasses the lower bound, the accuracy drops drastically. This phenomenon meets our expectation that slicing further on the base subnet loses too much fundamental basic representation, therefore hurts the accuracy significantly. In particular, the accuracy degradation is more evident in convolutional neural networks, where the correct representation depends heavily on the participant of all channels of the base network. In the experiments, we therefore evaluate lower bound 0.375 for reporting purpose, whose computational cost is roughly 14.1% of the full network respectively and empirically can be adjusted readily according to requirement.

5.2 NNLM for Language Modeling

5.2.1 Language modeling task and dataset

The task of language modeling is to model the probability distribution over a sequence of words. Neural Network

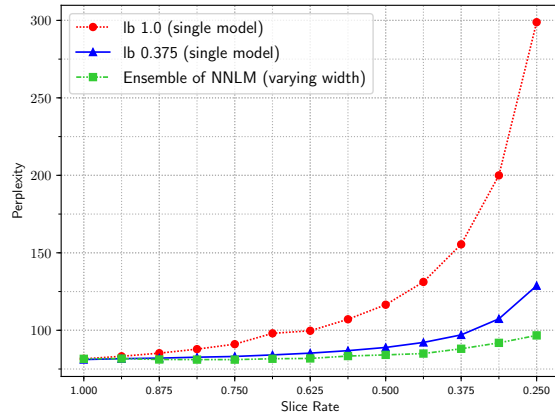


Figure 5: Results of NNLM trained w/o *model slicing*.

Language Model (NNLM) [38, 53, 39] specifies the distribution over next word w_{t+1} given the historical word sequence $w_{1:t} = [w_1, w_2, \dots, w_t]$ with neural networks. Training of NNLM involves minimizing the negative log-likelihood (NLL) of the sequence: $NLL = -\sum_{t=1}^T \log P(w_t | w_{1:t-1})$. Following the common practice for language modeling, we use perplexity (PPL) to evaluate the performance: $PPL = \exp(\frac{NLL}{T})$. We adopt the popular English Penn Tree Bank (PTB) dataset and use the standard train/test/validation split by [38].

5.2.2 NNLM configuration and training details

Following [38, 53, 39], the NNLM model in the experiments consists of an input embedding layer, two consecutive LSTM [18] layers, an output dense layer and finally a softmax layer. The embedding dimension is 650 and both LSTM layers contain 640 units. In addition, three dropout layers with dropout rate 0.5 follow the embedding and two LSTM layers. The models are trained by truncated back propagation through time for 35 time steps, minimizing NLL during training without any regularization terms using SGD with batch size 20. The learning rate is initially set to 20 and quartered in the next epoch if the perplexity does not decrease on the validation set. *Model slicing* applies to both recurrent layers and the output dense layer with output rescaling.

5.2.3 NNLM Results

Results in Figure 5 and Table 2 show that *model slicing* is effective to support on demand workload with one single model only at the cost of negligible performance loss. The performance of the network trained without *model slicing* decreases quickly. With *model slicing*, the performance stays rather close to the corresponding fixed models, which is typically the upper bound performance. In particular, the performance of the r -net is slightly better than the corresponding fixed model when the *slice rate* is near 1.0. For instance, as is shown in Table 2, the perplexity is 81.12 for the r -1 net and 81.58 for the full fixed model. This validates our hypothesis that the regularization and ensemble effect can improve the model performance. In addition, the student-teacher effect also facilitates the learning process

Table 1: Configurations of representative convolutional neural networks on CIFAR (left panel) and ImageNet (right panel) datasets. Building blocks are denoted as “[block, number of channels] \times number of blocks”.

Group	Output Size	VGG-13	ResNet-L-k	WRN-28-10	Output Size	VGG-16
conv1	32 \times 32	[conv3 \times 3, 64] \times 2	[B-Block, 16k] \times 1	[Block, 16] \times 1	112 \times 112	[conv3 \times 3, 64] \times 2
conv2	32 \times 32	-	[B-Block, 16k] \times N	[Block, 16 \times 10] \times 4	56 \times 56	[conv3 \times 3, 128] \times 2
conv3	16 \times 16	[conv3 \times 3, 128] \times 2	[B-Block, 32k] \times N	[Block, 32 \times 10] \times 4	28 \times 28	[conv3 \times 3, 256] \times 3
conv4	8 \times 8	[conv3 \times 3, 256] \times 2	[B-Block, 64k] \times N	[Block, 64 \times 10] \times 4	14 \times 14	[conv3 \times 3, 512] \times 3
conv5	8 \times 8	[conv3 \times 3, 512] \times 4	-	-	7 \times 7	[conv3 \times 3, 512] \times 3
avgPool/FC	1 \times 1	[avg8 \times 8, 512]	[avg8 \times 8, 64k \times 4]	[avg8 \times 8, 64 \times 10]	4096	[512 \times 7 \times 7, 4096, 4096]
Dataset	-	CIFAR	CIFAR	CIFAR	-	ImageNet-12
Params	-	9.41M	$\sim 1.72 \frac{k^2 L}{164}$ M	36.49M	-	138.36M

by transferring and sharing knowledge learned among these subnets.

Table 2: Remaining estimated percentage of computation (C_t), perplexity of NNLM on PTB w.r.t slice rate r .

Slice Rate r	1.000	0.875	0.750	0.625	0.500	0.375	0.250
C_t	100.0	76.56	56.25	39.06	25.00	14.06	6.250
NNLM-1.0	81.58	85.23	91.04	99.68	116.5	155.5	298.8
NNLM-0.375	81.12	82.02	83.10	85.25	88.92	97.02	128.8
NNLM-fixed	81.58	81.66	81.78	81.83	84.13	88.08	96.69

Another interesting finding is that the performance decreases relatively smoothly even after r surpasses the lower bound. This shows that in dense and recurrent layers, each basic component contributes relatively equally, and thus the network can still function normally with part of the components being removed.

5.3 CNNs for image classification

In this subsection, we evaluate *model slicing* on image classification tasks, mainly focusing on three representative types of convolutional neural networks. We first introduce dataset statistics for the evaluation. Then detailed configurations of the networks and training details are introduced. Finally, we compare and discuss the results of CNNs trained with *model slicing* comparing with the baselines.

5.3.1 Datasets

We evaluate the performance of CNNs with *model slicing* on CIFAR [29] and ImageNet-12 [11] image classification datasets.

The two CIFAR [29] datasets consist of 32×32 colors scenery images. CIFAR-10 (C10) consists of images drawn from 10 classes and CIFAR-100 (C100) from 100 classes. The training and testing sets for both datasets contain 50,000 and 10,000 images respectively. Following the standard data augmentation scheme [15, 24, 22], each image is first zero-padded with 4 pixels on each side, then randomly cropped to produce 32×32 images again, followed by a random horizontal flip. We normalize the data using the channel means and standard deviations for data pre-processing.

The ILSVRC 2012 image classification dataset contains 1.2 million images for training and another 50,000 for validation from 1000 classes. We adopt the same data augmentation scheme for training images following the convention [15, 52, 22], and apply a 224×224 center crop to images at test time. The results are reported on the validation set following common practice.

5.3.2 CNN Architectures and Training Details

Model slicing dynamically slices channels within each layer in CNNs, thus we adopt three architectures differing mainly in the channel width for evaluation. The first architecture is VGG [43] whose convolutional layer is a plain 3×3 conv of medium channel width. The second architecture is the pre-activation residual network [16]. ResNet is composed of the pre-activation bottleneck block [16], denoting as B-Block ($conv1 \times 1 - conv3 \times 3 - conv1 \times 1$) whose convolutional layer is relatively narrow with fewer channels. We evaluate *model slicing* on ResNet of varying depth and width, and denote the architecture adopted as ResNet-L-k, with L, k being the number of layers and widening factor [52] of the channel width for each layer. The third architecture is Wide Residual Network, which is also denoted as WRN-L-k. In WRN, we use the basic building block denoted as Block, containing two consecutive 3×3 conv. Detailed configurations of these three CNNs are listed in Table 1. To support *model slicing*, each convolutional layer and its coupling batch-norm layer is replaced with its *model slicing* counterpart coupled with a group-norm layer. For CIFAR datasets, we train 300 epochs on VGG-13 and ResNet-L-k, and 200 epochs on WRN-28-10 with SGD of batch size 128 and initial learning rate 0.1. For ImageNet, we train 90 epochs on VGG-16 with SGD of batch size 128 and initial learning rate 0.05. Other training details follow their original settings.

5.3.3 Results of Model Slicing on CNNs

Results of representative CNNs on CIFAR datasets are summarized in Figure 2 and Figure 6. Generally speaking, the accuracy of CNNs trained with *model slicing* is comparable to the corresponding fixed models, namely the ensemble of networks of varying width, with *slice rate* larger than lb . This phenomenon is more prominent for networks whose convolutional layers are wider, e.g. the VGG-13, WRN-28-10 and ResNet-L56-k2.

In Figure 2, we compare the accuracy of *model slicing* with more baseline methods in ResNet. We can observe that the accuracy of ResNet-164 trained with *model slicing* (single model L164-k1) surpasses ResNet with Multi-Classifiers baseline, especially in lower budget prediction. However, it has a noticeable accuracy gap compared to the ensemble of ResNet of varying width, which is mainly because each convolutional layer of ResNet-164 is narrow. For instance, each convolutional layer in conv1/conv2 comprises 16 channels (see Table 1) thus only 6 channels remain for prediction with *slice rate* 0.375, resulting in limited representational power. Therefore, *model slicing* works more effectively with wider convolutional layers which holds true for the majority of CNNs. With twice the channel width, ResNet-L56-k2 achieves performance close to the ensemble of varying

Table 3: Remaining estimated percentage of computation footprint (C_t), error rate of VGG-13 on CIFAR-10 and VGG-16 on ImageNet w.r.t slice rate r .

Slice Rate r	1.000	0.9375	0.8750	0.8125	0.7500	0.6875	0.6250	0.5625	0.500	0.4375	0.375	0.3125	0.2500
C_t	100.0%	87.89%	76.56%	66.02%	56.25%	47.27%	39.06%	31.64%	25.00%	19.14%	14.06%	9.77%	6.25%
VGG-13-1.0	5.626	8.110	12.45	18.37	32.07	42.04	55.82	73.09	78.63	83.65	87.77	89.73	89.81
VGG-13-0.375	5.650	5.800	5.840	5.870	5.780	5.910	6.120	6.680	7.440	7.74	8.620	28.14	65.23
VGG-13-fixed	5.626	5.766	5.894	6.068	6.084	6.142	6.208	6.600	6.614	6.894	7.148	7.690	8.374
VGG-16 top1	29.71	29.82	30.13	30.56	31.11	31.84	33.22	35.02	37.01	38.76	39.89	99.65	99.86
VGG-16 top5	10.47	10.44	10.69	10.92	11.30	11.70	12.40	13.52	15.01	15.35	16.71	98.64	99.27

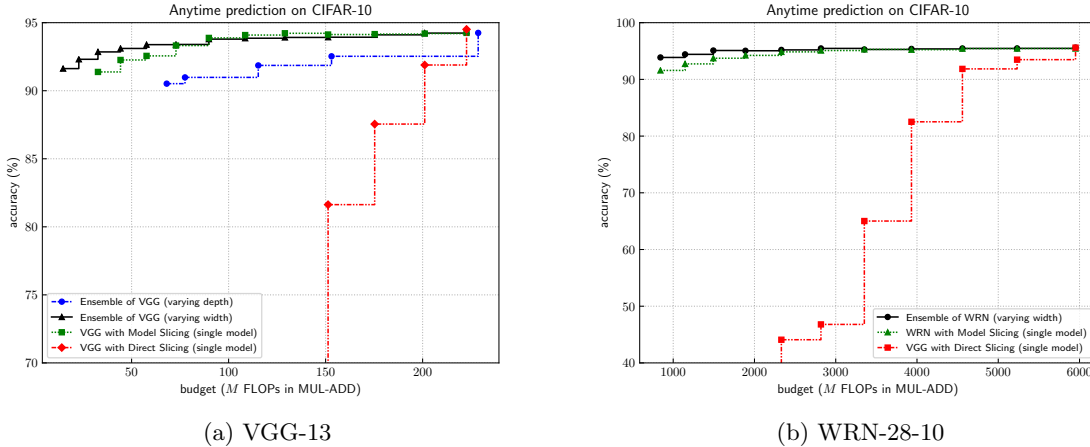


Figure 6: Performance of representative CNN architectures trained w/o *model slicing* on the CIFAR-10 dataset.

depth/width with only one model, which achieves higher accuracies than SkipNet [48] in corresponding inference budgets and furthermore, provides generally better and wider range of accuracy-budget trade-offs than MSDNet [21].

We can also notice in Figure 6 and Table 3 that the accuracy of CNNs trained conventionally (*lb* 1.0) decreases drastically as more channels are sliced off. This shows that channels within the same convolutional layer cooperate closely with each other such that excluding even a small fraction of these channels will spoil the representation of the network trained conventionally. With *model slicing*, however, we can get accuracy close to the ensemble of networks of varying width in one single network with far less memory and computational operation dynamically. For example, the error rate is 8.62% for VGG-13-0.375 (Table 3) when *slice rate* is 0.375, which costs only 14.06% of the computational operation of the full network ($\sim 7.11x$ computation acceleration). This claim is also supported by results of VGG-16 with *model slicing* on large dataset ImageNet in Table 3 that with *slice rate* being 0.375, the top-1 and top-5 error of VGG-16 is 39.89% and 16.71% respectively, which is still lower than 40.7% and 18.2% of AlexNet [30].

5.4 Visualization and Simulation

In this subsection, we reflect on the effect of *model slicing* training on neural networks, mainly focusing on convolutional neural networks, and visualize the training process.

5.4.1 Residual Learning Effect of Model Slicing

In CNNs trained with *model slicing*, each convolutional layer is followed by a group normalization layer to stabilize

the output scale with a scaling factor, formally γ in Equation 6. This scaling factor largely represents the importance of the corresponding channel. We thus visualize the evolution of these scaling factors in Figure 7. Specifically, we take first convolutional layers from conv3, conv4 and conv5 of VGG-13 (see Table 1), which corresponds to low, medium and high level feature extractors. We can notice an obvious stratified pattern in Figure 7. Groups from g_1 to g_6 in the base network gradually learn the largest scaling factor values. Meanwhile, from g_6 to g_{16} , the average scaling factor values also become smaller. This corroborates our assumption that *model slicing* training encourages residual learning, where the base network forms the most fundamental representation and following groups gradually build up the representation.

5.4.2 Learning Curves of Model Slicing

Figure 8 illustrates learning curves of VGG-13 trained with *model slicing* compared with the full fixed model. Learning curves of the subnets of VGG-13 trained with *model slicing* reveal that the error rate drops faster in larger subnets and smaller subnets follow closely to the corresponding larger subnets. This indicates the knowledge distillation effect, where larger subnets learn faster and gradually transfer the knowledge learned to smaller subnets. We can also notice that the accuracy of subnets of a relatively larger slice rate keeps close to the full fixed model, which means that *model slicing* can produce comparable results with significantly less memory and computation.

5.4.3 Prediction Consistency of Model Slicing

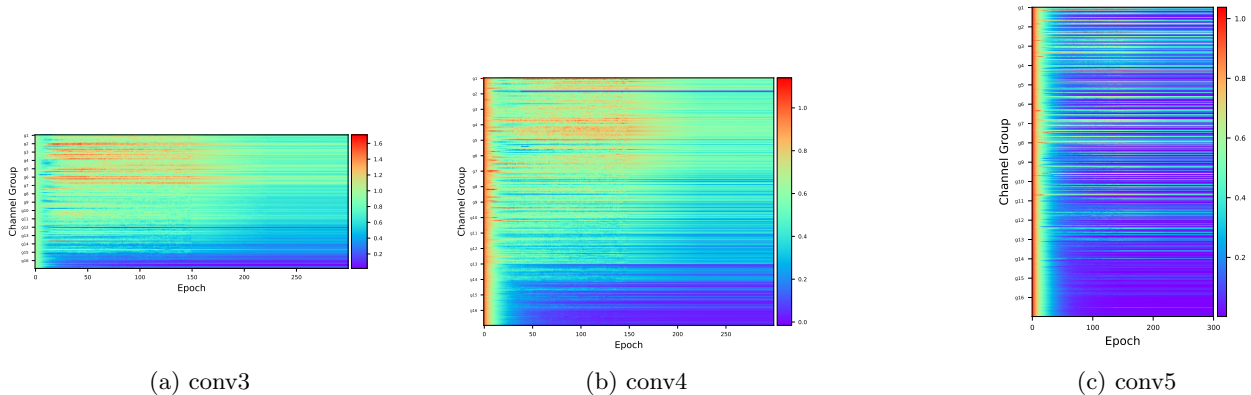


Figure 7: Visualization of channel scaling factors (γ from Equation 6) in scale as the training evolves, taken from the first convolutional layer of conv3, conv4, conv5 (Table 1) of VGG-13 trained on CIFAR-10 respectively. Brighter colors correspond to larger values.

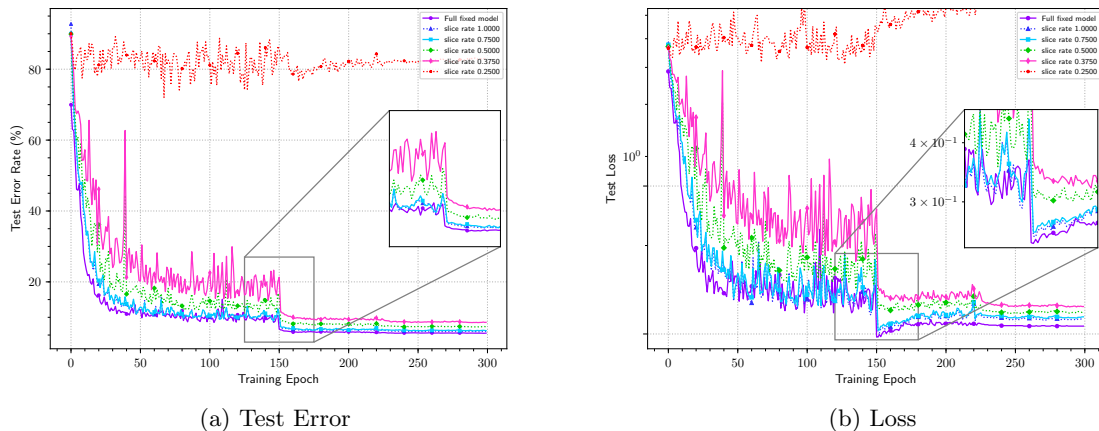


Figure 8: Test Error Rate and Loss curves of VGG-13 full fixed model and VGG-13 trained with *model slicing* (lb 0.375) validated under different *slice rate* on CIFAR-10 dataset.

We are also interested in the consistency of results given by *model slicing* with different slice rate. Naturally, the outputs by models with different slice rate are not the same. However, based on the design of *model slicing*, the model with a larger slice rate actually uses models with smaller slice rate as part of its model ensemble. Therefore, all the models are expected to share similar prediction, where models with larger slice rate could be able to correct some samples wrongly predicted by smaller models. Figure 9 shows the *inclusion coefficient* of wrongly predicted samples between each pair of models. Inclusion coefficient measures the ratio of wrongly predicted samples by the larger model which are also wrongly predicted by the smaller model. Essentially, it is a measurement on the ratio of errors overlapped with errors of other models. Unsurprisingly, the prediction behavior of *model slicing* is much more consistent than that of training different fixed models separately. Therefore, *model slicing* may not be feasible for applications such as model ensemble since it cannot provide much of diversity, but could

be extremely useful for applications requiring consistent prediction such as cascade ranking where the accumulated error is expected to be minimized.

5.4.4 Simulation of Cascade Ranking

We further simulate a cascade ranking scenario with 6 stages of classifiers. CIFAR-10 test dataset is adopted here for illustration which contains 10 types of items (classes) and 1000 items (images) for each type, and VGG-13 (see Table 1) is adopted as the base model. Each model (classifier) is required to correctly classify the type and keep those items for next stage processing. The baseline solution is cascade models of varying width r of the base model, and this is compared with our solution with corresponding cascade sub-models sliced from one full-width base model trained with *model slicing*. The parameter size and FLOPs for each single model is given in Table 4. The cascade ranking pipeline deploys smaller models in early stages to efficiently filter irrelevant items, and larger but more costly models in later

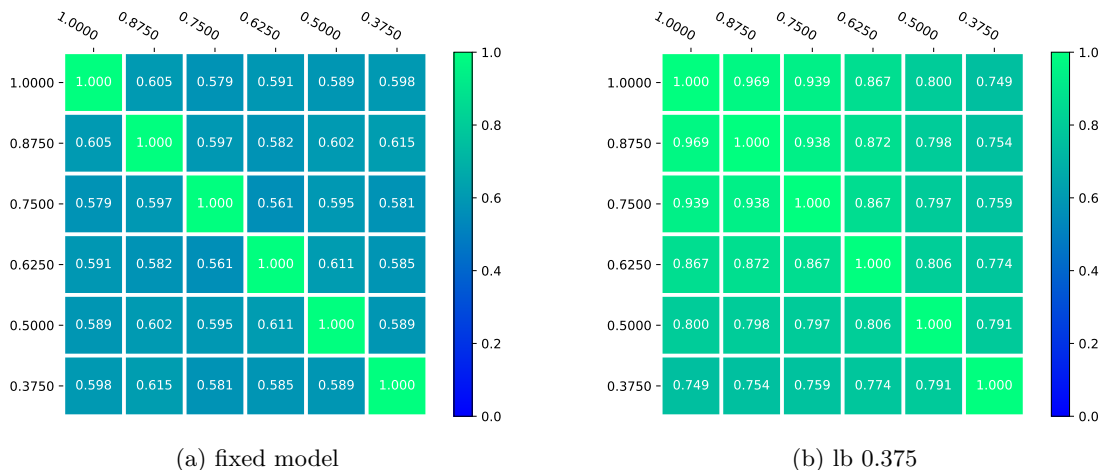


Figure 9: Heatmap of the *inclusion coefficient* of wrongly predicted samples between each pair of VGG-13 fixed models and sliced subnets of VGG-13 trained with *model slicing* (lb 0.375) respectively on CIFAR-10 dataset.

stages for higher prediction quality.

Table 4: Simulation of cascade ranking with cascade of varying width models and model trained with *model slicing*.

model width r	0.375	0.500	0.625	0.750	0.875	1.000
Params (M)	1.33	2.36	3.68	5.30	7.21	9.42
FLOPs (M)	32.66	57.70	89.82	129.01	175.29	222.64
model cascade	92.85% 9285	93.39% 9017	93.79% 8866	93.92% 8749	94.11% 8676	94.37% 8609
model slicing	91.38% 9138	92.56% 8985	93.88% 8909	94.22% 8875	94.16% 8868	94.35% 8867

Table 4 summarizes the main results of precision and also the aggregate recall of correct type in each stage. There are two main advantages of the *model slicing* solution over conventional cascade model solution: first, in terms of effectiveness, the *model slicing* solution obtains 8867 correct items comparing to 8609 of the conventional solution. The significantly more correct item recall is mainly due to the better prediction consistency; second, in terms of efficiency, the conventional solution takes totally 29.30M parameters and 707.12M FLOPs computation for each item, while *model slicing* solution only takes 9.42M parameters in one model and close to 222.64M FLOPs computation thanks to the computation reuse discussed in Section 3.4.

6. CONCLUSIONS

There are relatively few efforts devoted to neural networks providing predictions within dynamic memory and computational operation budget. In this paper, we propose *model*

slicing, a general training and inference framework supporting elastic inference cost for neural networks. The key idea of *model slicing* is to impose structural constraint to basic components each layer and regulate the width of the network with *slice rate*. We have provided detailed analysis and discussion on training details of *model slicing* and evaluated *model slicing* through extensive experiments.

Results on NLP and vision tasks show that neural networks trained with *model slicing* can effectively support on demand workload by slicing a subnet from the trained network dynamically. With *model slicing*, neural networks can achieve significant runtime memory and computational operation reduction with minor performance degeneration, e.g. 7.11x with *slice rate* 0.375. Unlike conventional model compression methods where the computation reduction is limited, the computation operation required decreases quadratically to *slice rate*.

Model slicing also provides some insights into the learning process of neural networks. Networks trained with *model slicing* encourages residual learning each layer, where components in the base network learn fundamental representation while appending components build up residual representation gradually. Meanwhile, the learning process is reminiscent of knowledge distillation. During training, larger subnets learn faster and gradually transfer the knowledge learned to smaller subnets. Lastly, *model slicing* can be adapted readily to model compression scenario by slicing a proper subnet.

7. REFERENCES

- [1] M. Boehm, M. W. Dusenberry, D. Eriksson, A. V. Evfimievski, F. M. Manshadi, N. Pansare, B. Reinwald, F. R. Reiss, P. Sen, A. C. Surve, et al. Systemml: Declarative machine learning on spark. *Proceedings of the VLDB Endowment*, 9(13):1425–1436, 2016.
- [2] W. Cao, Y. Gao, B. Lin, X. Feng, Y. Xie, X. Lou, and P. Wang. Tcprt: Instrument and diagnostic analysis system for service quality of cloud databases at massive scale in real-time. In *Proceedings of the 2018 International Conference on Management of Data*, pages 615–627. ACM, 2018.
- [3] S. Changpinyo, M. Sandler, and A. Zhmoginov. The power of sparsity in convolutional neural networks. *arXiv preprint arXiv:1702.06257*, 2017.
- [4] S. Chaudhuri, B. Ding, and S. Kandula. Approximate query processing: No silver bullet. In *Proceedings of the 2017 ACM SIGMOD International Conference on Management of Data*, pages 511–519. ACM, 2017.
- [5] R.-C. Chen, L. Gallagher, R. Blanco, and J. S. Culpepper. Efficient cost-aware cascade ranking in multi-stage retrieval. In *Proceedings of the 40th International ACM SIGIR Conference on Research and Development in Information Retrieval*, pages 445–454. ACM, 2017.
- [6] T. Chen and C. Guestrin. Xgboost: A scalable tree boosting system. In *Proceedings of the 22nd acm sigkdd international conference on knowledge discovery and data mining*, pages 785–794. ACM, 2016.
- [7] W. Chen, J. Wilson, S. Tyree, K. Weinberger, and Y. Chen. Compressing neural networks with the hashing trick. In *International Conference on Machine Learning*, pages 2285–2294, 2015.
- [8] K. Cho, B. Van Merriënboer, D. Bahdanau, and Y. Bengio. On the properties of neural machine translation: Encoder-decoder approaches. *arXiv preprint arXiv:1409.1259*, 2014.
- [9] F. Chollet. Xception: Deep learning with depthwise separable convolutions. *arXiv preprint*, pages 1610–02357, 2017.
- [10] M. Courbariaux, I. Hubara, D. Soudry, R. El-Yaniv, and Y. Bengio. Binarized neural networks: Training deep neural networks with weights and activations constrained to +1 or -1. *arXiv preprint arXiv:1602.02830*, 2016.
- [11] J. Deng, W. Dong, R. Socher, L.-J. Li, K. Li, and L. Fei-Fei. Imagenet: A large-scale hierarchical image database. In *Computer Vision and Pattern Recognition, 2009. CVPR 2009. IEEE Conference on*, pages 248–255. Ieee, 2009.
- [12] E. L. Denton, W. Zaremba, J. Bruna, Y. LeCun, and R. Fergus. Exploiting linear structure within convolutional networks for efficient evaluation. In *Advances in neural information processing systems*, pages 1269–1277, 2014.
- [13] S. Han, H. Mao, and W. J. Dally. Deep compression: Compressing deep neural networks with pruning, trained quantization and huffman coding. *arXiv preprint arXiv:1510.00149*, 2015.
- [14] S. Han, J. Pool, J. Tran, and W. Dally. Learning both weights and connections for efficient neural network. In *Advances in neural information processing systems*, pages 1135–1143, 2015.
- [15] K. He, X. Zhang, S. Ren, and J. Sun. Deep residual learning for image recognition. In *Proceedings of the IEEE conference on computer vision and pattern recognition*, pages 770–778, 2016.
- [16] K. He, X. Zhang, S. Ren, and J. Sun. Identity mappings in deep residual networks. In *European conference on computer vision*, pages 630–645. Springer, 2016.
- [17] G. Hinton, O. Vinyals, and J. Dean. Distilling the knowledge in a neural network. *arXiv preprint arXiv:1503.02531*, 2015.
- [18] S. Hochreiter and J. Schmidhuber. Long short-term memory. *Neural computation*, 9(8):1735–1780, 1997.
- [19] A. G. Howard, M. Zhu, B. Chen, D. Kalenichenko, W. Wang, T. Weyand, M. Andreetto, and H. Adam. Mobilenets: Efficient convolutional neural networks for mobile vision applications. *arXiv preprint arXiv:1704.04861*, 2017.
- [20] H. Hu, D. Dey, M. Hebert, and J. A. Bagnell. Learning anytime predictions in neural networks via adaptive loss balancing. 2018.
- [21] G. Huang, D. Chen, T. Li, F. Wu, L. van der Maaten, and K. Q. Weinberger. Multi-scale dense convolutional networks for efficient prediction. *CoRR*, abs/1703.09844, 2, 2017.
- [22] G. Huang, Z. Liu, K. Q. Weinberger, and L. van der Maaten. Densely connected convolutional networks. *arXiv preprint arXiv:1608.06993*, 2016.
- [23] G. Huang, Z. Liu, K. Q. Weinberger, and L. van der Maaten. Densely connected convolutional networks. In *Proceedings of the IEEE conference on computer vision and pattern recognition*, volume 1, page 3, 2017.
- [24] G. Huang, Y. Sun, Z. Liu, D. Sedra, and K. Q. Weinberger. Deep networks with stochastic depth. In *European Conference on Computer Vision*, pages 646–661. Springer, 2016.
- [25] F. N. Iandola, S. Han, M. W. Moskewicz, K. Ashraf, W. J. Dally, and K. Keutzer. Squeezenet: Alexnet-level accuracy with 50x fewer parameters and 0.5 mb model size. *arXiv preprint arXiv:1602.07360*, 2016.
- [26] S. Ioffe and C. Szegedy. Batch normalization: Accelerating deep network training by reducing internal covariate shift. *arXiv preprint arXiv:1502.03167*, 2015.
- [27] D. Kang, J. Emmons, F. Abuzaid, P. Bailis, and M. Zaharia. Noscope: optimizing neural network queries over video at scale. *Proceedings of the VLDB Endowment*, 10(11):1586–1597, 2017.
- [28] G. Ke, Q. Meng, T. Finley, T. Wang, W. Chen, W. Ma, Q. Ye, and T.-Y. Liu. Lightgbm: A highly efficient gradient boosting decision tree. In *Advances in Neural Information Processing Systems*, pages 3146–3154, 2017.
- [29] A. Krizhevsky and G. Hinton. Learning multiple layers of features from tiny images. Technical report, Citeseer, 2009.
- [30] A. Krizhevsky, I. Sutskever, and G. E. Hinton. Imagenet classification with deep convolutional neural

- networks. In *Advances in neural information processing systems*, pages 1097–1105, 2012.
- [31] A. Kumar, R. McCann, J. Naughton, and J. M. Patel. Model selection management systems: The next frontier of advanced analytics. *ACM SIGMOD Record*, 44(4):17–22, 2016.
- [32] G. Larsson, M. Maire, and G. Shakhnarovich. Fractalnet: Ultra-deep neural networks without residuals. *arXiv preprint arXiv:1605.07648*, 2016.
- [33] F. Li, B. Wu, K. Yi, and Z. Zhao. Wander join: Online aggregation via random walks. In *Proceedings of the 2016 International Conference on Management of Data*, pages 615–629. ACM, 2016.
- [34] H. Li, A. Kadav, I. Durdanovic, H. Samet, and H. P. Graf. Pruning filters for efficient convnets. *arXiv preprint arXiv:1608.08710*, 2016.
- [35] S. Liu, F. Xiao, W. Ou, and L. Si. Cascade ranking for operational e-commerce search. In *Proceedings of the 23rd ACM SIGKDD International Conference on Knowledge Discovery and Data Mining*, pages 1557–1565. ACM, 2017.
- [36] Z. Liu, J. Li, Z. Shen, G. Huang, S. Yan, and C. Zhang. Learning efficient convolutional networks through network slimming. In *Computer Vision (ICCV), 2017 IEEE International Conference on*, pages 2755–2763. IEEE, 2017.
- [37] L. McIntosh, N. Maheswaranathan, D. Sussillo, and J. Shlens. Recurrent segmentation for variable computational budgets. *arXiv preprint arXiv:1711.10151*, 2017.
- [38] T. Mikolov, M. Karafiát, L. Burget, J. Černocký, and S. Khudanpur. Recurrent neural network based language model. In *Eleventh Annual Conference of the International Speech Communication Association*, 2010.
- [39] O. Press and L. Wolf. Using the output embedding to improve language models. *arXiv preprint arXiv:1608.05859*, 2016.
- [40] M. Richardson, E. Dominowska, and R. Ragno. Predicting clicks: estimating the click-through rate for new ads. In *Proceedings of the 16th international conference on World Wide Web*, pages 521–530. ACM, 2007.
- [41] N. Shazeer, A. Mirhoseini, K. Maziarz, A. Davis, Q. Le, G. Hinton, and J. Dean. Outrageously large neural networks: The sparsely-gated mixture-of-experts layer. *arXiv preprint arXiv:1701.06538*, 2017.
- [42] X. Shi, B. Cui, G. Dobbie, and B. C. Ooi. Towards unified ad-hoc data processing. In *Proceedings of the 2014 ACM SIGMOD International Conference on Management of Data*, pages 1263–1274. ACM, 2014.
- [43] K. Simonyan and A. Zisserman. Very deep convolutional networks for large-scale image recognition. *arXiv preprint arXiv:1409.1556*, 2014.
- [44] S. Srinivas, A. Subramanya, and R. V. Babu. Training sparse neural networks. *arXiv preprint arXiv:1611.06694*, 2016.
- [45] A. Veit, M. J. Wilber, and S. Belongie. Residual networks behave like ensembles of relatively shallow networks. In *Advances in Neural Information Processing Systems*, pages 550–558, 2016.
- [46] L. Wang, J. Lin, and D. Metzler. A cascade ranking model for efficient ranked retrieval. In *Proceedings of the 34th international ACM SIGIR conference on Research and development in Information Retrieval*, pages 105–114. ACM, 2011.
- [47] X. Wang, Y. Luo, D. Crankshaw, A. Tumanov, F. Yu, and J. E. Gonzalez. Idk cascades: Fast deep learning by learning not to overthink. *arXiv preprint arXiv:1706.00885*, 2017.
- [48] X. Wang, F. Yu, Z.-Y. Dou, and J. E. Gonzalez. Skipnet: Learning dynamic routing in convolutional networks. *arXiv preprint arXiv:1711.09485*, 2017.
- [49] W. Wen, C. Wu, Y. Wang, Y. Chen, and H. Li. Learning structured sparsity in deep neural networks. In *Advances in Neural Information Processing Systems*, pages 2074–2082, 2016.
- [50] Y. Wu and K. He. Group normalization. *CoRR*, abs/1803.08494, 2018.
- [51] S. Xie, R. Girshick, P. Dollár, Z. Tu, and K. He. Aggregated residual transformations for deep neural networks. In *Computer Vision and Pattern Recognition (CVPR), 2017 IEEE Conference on*, pages 5987–5995. IEEE, 2017.
- [52] S. Zagoruyko and N. Komodakis. Wide residual networks. *arXiv preprint arXiv:1605.07146*, 2016.
- [53] W. Zaremba, I. Sutskever, and O. Vinyals. Recurrent neural network regularization. *arXiv preprint arXiv:1409.2329*, 2014.
- [54] C. Zhang, A. Kumar, and C. Ré. Materialization optimizations for feature selection workloads. *ACM Transactions on Database Systems (TODS)*, 41(1):2, 2016.
- [55] X. Zhang, X. Zhou, M. Lin, and J. Sun. Shufflenet: An extremely efficient convolutional neural network for mobile devices. *arXiv preprint arXiv:1707.01083*, 2017.
- [56] Y. Zhang, W. Zhang, and J. Yang. I/o-efficient statistical computing with riot. In *Data Engineering (ICDE), 2010 IEEE 26th International Conference on*, pages 1157–1160. IEEE, 2010.
- [57] L. Zheng, L. Shen, L. Tian, S. Wang, J. Wang, and Q. Tian. Scalable person re-identification: A benchmark. In *Proceedings of the IEEE International Conference on Computer Vision*, pages 1116–1124, 2015.